Adaptation of Central Metabolite Pools to Variations in Growth Rate and Cultivation Conditions in Saccharomyces Cerevisiae

Kanhaiya Kumar
Norwegian University of Science and Technology: Norges teknisk-naturvitenskapelige universitet
Vishwesh Venkatraman
Norwegian University of Science and Technology: Norges teknisk-naturvitenskapelige universitet
Per Bruheim (Per.Bruheim@ntnu.no)
Norges teknisk-naturvitenskapelige universitet https://orcid.org/0000-0002-7851-8083

Research

Keywords: Metabolomics, Bioreactor, Chemostat, Mass Spectrometry, Yeast, Glycolysis, Physiology

Posted Date: December 1st, 2020

DOI: https://doi.org/10.21203/rs.3.rs-113855/v1

Version of Record: A version of this preprint was published at Microbial Cell Factories on March 9th, 2021. See the published version at https://doi.org/10.1186/s12934-021-01557-8.

Adaptation of central metabolite pools to variations in growth rate and cultivation conditions in *Saccharomyces cerevisiae*

Kanhaiya Kumar[1], Vishwesh Venkatraman[2], and Per Bruheim[1]*

[1] Department of Biotechnology and Food Science, Norwegian University of Science and Technology (NTNU), 7491, Trondheim, Norway

[2] Department of Chemistry, Norwegian University of Science and Technology (NTNU), 7491, Trondheim, Norway

*** Correspondence:**
Corresponding Author
Per.Bruheim@ntnu.no

Keywords: Metabolomics, Bioreactor, Chemostat, Mass Spectrometry, Yeast, Glycolysis, Physiology

ABSTRACT

Background: *Saccharomyces cerevisiae* is a well-known popular model system for basic biological studies and to serve as host organism for heterologous production of commercially interesting small molecules and proteins. The central metabolism is at the core to provide building blocks and energy to support growth and survival in normal situations as well as during exogeneous stresses and forced heterologous protein production. Here, we present a comprehensive study of intracellular central metabolite pool profiling when growing *S. cerevisiae* on different carbon sources in batch cultivations and at different growth rates in nutrient limited glucose chemostats. Latest versions of absolute quantitative mass spectrometry-based metabolite profiling methodology were applied to cover glycolytic and pentose phosphate pathway metabolites, TCA, complete amino acid and deoxy-/nucleoside phosphate pools. We have attempted to correlate the total metabolite pool composition with growth rates and nutrient limitation in both batch and chemostat cultivations. We have also tried to dissect the Crabtree-effect, i.e. ethanol-producing cultivation conditions, based on metabolite pool composition.

Results: Glutamate, glutamine, alanine and citrate were the four most abundant metabolites for most conditions tested. Amino acid is the dominant metabolite class even though a marked relative reduction compared to the other metabolite classes was observed for nitrogen and phosphate limited chemostats. Interestingly, glycolytic and PPP metabolites display largest variation among the cultivation conditions while the nucleoside phosphate pools are more stable and vary within a closer concentration window. The overall trends for glucose and nitrogen limited chemostats were increased metabolite pools with increasing growth rate. Next, comparing the chosen chemostat reference growth rate (0.12 h^{-1}, approximate one-fourth of maximal unlimited growth rate) illuminates an interesting pattern: almost all pools are lower in nitrogen and phosphate limited conditions compared to glucose limitation, except for the TCA metabolites citrate, isocitrate and α-ketoglutarate.

Conclusions: This study provides new knowledge how the central metabolism is adapting to various cultivations conditions and growth rates which is essential for expanding our understanding of cellular metabolism and development of improved phenotypes in metabolic engineering.

BACKGROUND

Saccharomyces cerevisiae is a well-known popular model system for basic biological studies. It is also of considerable industrial interest, ranging from traditional bioprocesses of beer and wine production to serve as a host organism for heterologous production of commercially interesting small molecules and proteins. *S. cerevisiae* is a respiro-fermentative microorganism with characteristics of having the long-term Crabtree positive effect, which can produce ethanol under aerobic conditions, when fed with a high glucose concentration[1]. A high level of glucose represses the tricarboxylic acid (TCA) cycle and respiration, and pyruvate can overflow to ethanol through the high capacity pyruvate decarboxylase and constricted flux through pyruvate dehydrogenase[2]. Thus, this species can maintain active metabolism and growth under many different cultivation conditions. In this report, we explore how the central metabolite pools of *S. cerevisiae* adjust to the growth rate and cultivation conditions, a topic that has only been partly addressed in the literature.

The analysis of the metabolome - metabolomics - has gone through a remarkable instrumental and methodological development during the last two decades. NMR and mass spectrometry (MS) are the two main detection technologies used, the latter with superior properties for highly sensitive and comprehensive coverage of the metabolome. The MS-metabolomics workflow still faces major challenges in all steps, especially high recovery sampling and sample processing is a long-standing non-resolved topic. Besides, the mass spectrometer is a challenging detector when used for absolute quantification purposes[3]. Regardless, high-quality metabolome studies are continuously reported, adding new knowledge to biological function and mechanisms but are also used for guidance and evaluation in metabolic engineering projects[4-6]. Most studies are designed and interpreted at a relative scale, i.e. mutant vs. wild-type/ reference strains, but the ultimate goal is to report absolute intracellular concentrations[7]. Such information is essential to testing and validating

kinetic models[8], to increase of understanding in genotype-phenotype interactions and cellular engineering[9-11]. These data will be important for further emphasis to integrate different level omics-data with mathematical models, especially genome-scale metabolic models, of biological systems.

The available metabolome databases (e.g. E. coli/ Yeast, Human metabolome databases) contain an impressive collection of metabolite data but considerably lower amounts of information on intracellular concentrations[12-14]. Importantly, concentration entries can range several orders of magnitude for some metabolites. This may be attributed to the fact that different methodologies have been applied by different labs and are also under continuous development. Furthermore, sampling is often performed on cells grown under different conditions and in different physiological states. The metabolomics community has undertaken efforts to standardize metabolomics workflows[15], and an initiative to select a few model organisms to advance the field of Metabolomics [16].

Our group has developed a set of quantitative LC-MS/MS methods for central metabolism, all methods using ^{13}C-Isotope dilution strategy for highest level of quantitative precision and accuracy [17-19]). The core metabolism is centered on the glycolytic and pentose pathways, TCA and energy conserving mechanisms. Important metabolite classes are sugar phosphates and other phosphorylated metabolites, TCA organic acids and pyruvate and excreted metabolites like ethanol, lactic and acetic acids, amino acids, nucleoside mono-/di-/tri-phosphates. These pathways and metabolites not only serve to make energy available but also act as a precursor for macromolecular synthesis and are particularly interesting to monitor. We have applied this methodology in a previous study to report absolute intracellular concentration of several popular microbial and mammalian model systems, using early exponential growth phase as the reference physiological state [20].

Now, we turn the focus on central metabolite pools in bakers's yeast and how the composition varies with growth rate and cultivation condition. It has been known for many decades that macromolecular composition varies with growth rate[21], but there is limited information on how central metabolite pools are adjusted with growth rate. For our study we chose to use the frequently investigated *S. cerevisiae* cen.pk strain[22]. Boer and co-workers ran a series of metabolite profiling of yeast at steady-state in chemostats and

varied both growth rate and nutrient limitations[23]. They reported strong correlation in responses on metabolite concentration to nutrient limitations. Christen and Sauer performed a combined metabolome and fluxome study on seven yeast species, incl. *S. cerevisiae*[2]. They found the metabolite pool compositions to be mainly species specific, but, interestingly, an overarching-species metabolic flux correlation for fructose-1,6-diphosphate and dihydroxyacetone-phosphate was found. Most metabolome studies on yeast do not report absolute concentration and focus on using metabolite profiling in strain development and stress-situations, e.g. de Ruijer and co-workers used a quantitative metabolomics approach for study the metabolic burden of recombinant antibody production in *S. cerevisiae* [9], Nishino and co-workers investigated *S. cerevisiae* strains lacking PFK1 and ZWF1 using absolute quantitative methodology[24], Jung and co-workers used intracellular metabolite profiling for characterization of adaptation of *S. cerevisiae* to furfural stress[25]. These high-quality studies provide interesting information how yeast cells adapt to genetic changes and stress exposure. One challenge for such studies is how to interpret the metabolite data if a mutant strain is growing at different growth rate than the wild-type and if the stress exposure causes changes in growth rates. It might be that the resulting metabolite profiles are more consequences of the adaptation to changes of growth rate rather than the direct effect of the stress. A deeper insight into cellular adaptation at the central metabolome level to growth rate is highly needed, from a basic scientific point of view but also as guide for interpretation of other Metabolome studies. This is the background and motivation to undertake the present study in the model organism *S. cerevisiae*. Both batch (exponential and stationary phase) and chemostats (glucose, nitrogen and phosphate limited) at a series of dilution rates i.e. growth rates, were included since both bioreactor modes of operation are relevant in yeast physiology studies. We included also high dilution rates of the chemostats since we wanted to study the transition from nutrient limitation to unlimited growth. We envision that more studies, both inter-/ intra-species and with variable cultivation condition incl. various stress testing, should follow.

RESULTS

The outline of the Results section is first to present the cultivation data as they are important constraints on the evaluation and interpretation of the intracellular metabolite pool data. This is followed by the presentation of the absolute concentration of all individual metabolites across all sampling conditions and next pooled into the respective metabolite groups. Further, a series of multivariate analyses were done, both on complete data set and within one-variable conditions. Finally, more closer inspections with pairwise comparisons are performed.

Cultivation data

Batch cultivation on glucose, fructose, galactose, and sucrose. The growth performance of *S. cerevisiae* CEN.PK on glucose, fructose and sucrose (GluFruSuc) were nearly similar as indicated by different growth parameters such as biomass yield on substrate, specific growth rate, specific CO_2 evolution rate, specific substrate uptake rate (Figure 1A, tabulated data can be found in Supplementary Table S1). The exponential phase lasted 7 to 8 hours on all three carbon sources using the traditional yeast mineral medium with 15 g carbon source L^{-1} (see Supplementary Figure S1 for online CO_2 and O_2 offline gas profiles) introduced by Verduyn and co-workers (Verduyn et al., 1992)**.** The specific growth rates (μ) on glucose, fructose and sucrose were nearly similar having values 0.43 h^{-1}, 0.42 h^{-1}, 0.41 h^{-1}, respectively. Sucrose was hydrolyzed into glucose and fructose during the cultivation, and it was not detected in the broth after three hours of cultivation. Like several previous reports, glucose was preferentially consumed over fructose, which led to an initial build-up of fructose and the presence of fructose in broth even after consumption of glucose. This may be the reason for a nearly similar growth performance on sucrose as compared to fructose and glucose. Our result is corroborated with previous studies on this strain, e.g. van Dijken and co-workers reported μ of 0.41 h^{-1} and

biomass yield of 0.12 g biomass g^{-1} on glucose and μ of 0.38 h^{-1} on sucrose in shake flasks[22]. The growth performance on galactose was contrasted by a 13h long exponential phase, lower specific maximum growth rate of 0.26 h^{-1}, low galactose uptake rate, low release of fermentative products as ethanol, low CO_2 evolution and O_2 consumption rate compared to GluFruSuc (Figure 1A). However, the biomass yield was 0.26 g g^{-1} DCW after exponential phase, which was nearly two-fold higher compared to biomass yield after exponential phase on GluFruSuc. This growth performance is similar as previously reported[26]. *S. cerevisiae* CEN.PK is a Crabtree-positive strain and trace amounts of acetic acid, glycerol, succinic acid and α-ketoglutarate (neither reported) were also detected in addition to ethanol. The exponential aerobic respiratory-fermentative growth phase on sugars were succeeded with re-uptake and catabolism of ethanol as shown in earlier studies on glucose[22]. Metabolite profiling was performed in this phase also for three sugars (GluFruSuc).

Chemostats are strict nutrient-limited over the range of dilution rates with constant biomass yield[27]. For this study we also chose to increase the dilution rate above this threshold and approaching maximum growth rate and wash out situation. During this phase is the concentration of limited nutrient increasing and biomass concentration decreasing. Extracellular and metabolome samplings were performed after four to six volume exchanges where all monitoring parameters were stable (except highest dilution rate for phosphate limited).

The carbon (glucose) limited chemostat was operated in two different inlet glucose concentrations: low glucose (LG, feed glucose concentration of 1 g L^{-1}) and high glucose (HG, feed glucose concentration of 10 g L^{-1}) but still the limiting nutrient (Figures 1B and C, tabulated data can be found in Supplementary Tables S2 and S3). The highest tested dilution rate (0.41 h^{-1}) on HG chemostat approaches maximum specific growth rate but washout was not observed. Biomass yields was constant and at maximum for the two lowest dilution rates (0.12 and 0.24 h^{-1}) and by-product formation was negligible). The respiratory quotient (RQ) was close to one which indicates fully respiratory growth. This was corroborated with previous results where a decrease in glucose uptake rates were found to decrease in the secretion of the main fermentative product ethanol[2,22,28]. The threshold for onset of the Crabtree effect seems to be between specific growth rates of 0.26 h^{-1} and 0.35

h^{-1} and approaching same ethanol yields (Y_{EtOHS}) as the unlimited batch cultivation on glucose. Threshold specific growth rate can be defined as specific growth rate where yeast start to show respiro-fermentative growth. The Crabtree effect is usually discussed as a sugar concentration dependent effect and induced at higher concentrations, but in HG chemostat at μ=0.35 h^{-1}, most of the glucose was consumed, indicating that higher growth rates/ glucose consumption rates trigger this overflow mechanism also and not only high sugar concentrations. An increased specific glucose uptake rate enhances the glycolytic flux, which results into the diversion of pyruvate to both directions: TCA cycle and fermentative routes. This was also indicated by a high RQ at higher dilution rates. The RQ value higher than one indicates the diversion of pyruvate towards fermentative routes where one mole of pyruvate is consumed to produce one mole of carbon dioxide and one mole of ethanol without consuming oxygen. The appearance of ethanol was reported to be the most sensitive indicator for the onset of respiro-fermentative metabolism (van Dijken et al., 2000). In any case, this series of growth rates are interesting to study at the intracellular metabolite pool levels to monitor adaptation from fully aerobic to respiro-fermentative metabolism. Growth parameters of LG chemostats were same as HG chemostats for comparable dilution rates (Supplementary Tables S2 and S3). Ethanol was not detected at the highest dilution rate 0.31 h^{-1} which indicate that onset of the Crabtree effect is close to 0.35 h^{-1} in glucose limited chemostats, while ethanol production was observed in galactose batch cultivation at μ = 0.26 h^{-1}.

The nitrogen (ammonium) limited chemostat was operated in the range of dilution rates of 0.06 to 0.34 h^{-1} and contrary to carbon limitation, entire growth rate range was respiro-fermentative in nature (Figure 1D, tabulated data can be found in Supplementary Table S4**)**. The steady state biomass and ethanol concentration had a decreasing trend with an increase in the dilution rate while the glucose concentration in the outlet was increased with the dilution rate. However, on specific rate basis there is an increased ethanol yield. Also, the increase in dilution rate led to enhancement of specific respiration rate and RQ. The contribution of CO_2 in the carbon recovery was increased at higher dilution rates while the carbon recovery was mostly dominated by biomass and ethanol production at lower dilution rates. The specific glucose uptake

rate was higher in nitrogen than glucose limited chemostats at same dilution rates which indicates a higher catabolic activity of glucose when this nutrient is not limited.

The phosphorous (phosphate) limited chemostat was operated in the dilution rate of 0.06 h^{-1}, 0.12 h^{-1}, 0.18 h^{-1}. However, a steady state off gas composition was not observed at 0.18 h^{-1} after 4-6 volume exchanges though the culture was almost stable in terms of optical density. Like nitrogen limited chemostat, the phosphate limited chemostat had a higher specific glucose uptake rate, RQ and excretion of fermentative products in comparison of glucose limited chemostat (Figure 1E, tabulated data can be found in Supplementary Table S5). Ethanol production was also observed at all dilution rates, and, interestingly, a higher specific glucose consumption rate and ethanol yield were observed for the phosphate limited vs. nitrogen and glucose at the same growth rate (0.12 h^{-1}).

In all, our data reproduces previous reports where similar conditions were tested, and in addition we included conditions where chemostat dilution rates approaches maximum growth rate. All these extracellular substrate consumption and production formation rates are important data for the interpretation of the endometabolome data presented next.

Quantitative profiling of intracellular metabolite pools

Absolute intracellular concentration (in µmole/ g DW units) of all quantified metabolites across different cultivation conditions are shown in a logarithmic scaled heat-map (Figure 2, numbers are given in Supplementary Table S6) with corresponding relative standard deviations enclosed in Supplementary Figure S2 (also in numbers in Supplementary Table S6). At first glance the overall picture indicates a large degree of similarities in the metabolite pools, i.e. high abundant amino acids, low abundant deoxy nucleotides, but when summarizing individual metabolite pools into respective metabolite classes a relatively large variation is detected (Figure 3). First, there is a quite large difference in total metabolite pools with highest in glucose-limited chemostats (Figure 3, upper panel), and on a fractional scale the phosphate and nitrogen-limited chemostats stands out with relatively lower amino acid pools and higher TCA pools (Figure 3, lower panel).

There is also a trend with increased total pools with growth rate for glucose and nitrogen limited chemostats. Closing in at the individual molecule level is, as expected, a large range of concentrations observed (Supplementary Figure S3, left panel) as earlier indicated in the heatmap of Figure 2. Glutamate, glutamine, alanine and citrate are the four most abundant metabolites. Interestingly, glycolytic and PPP metabolites display largest variation among the cultivation conditions while the nucleoside phosphate pools display least variations (Supplementary Figure S3, right panel). At this coarse level of interpretation there is no inconspicuous correlation between different batch and chemostat cultivations nor Crabtree-effect, i.e ethanol producing cultivation conditions (all batch, all N- and P-limited chemostats and high dilutions rate C-limited chemostats) and overall metabolite pool composition.

Multivariate analysis. Submitting the total data set to PCA revealed a clear clustering of glucose-limited chemostats at all dilution rates vs. the other conditions along PC1 of the scores plot, while GluFruSuc batch cultivations are separated from N-/ P lim chemostats along PC2 (Supplementary Figure S4, upper panel). Interestingly, the galactose batch is closer to N-/P lim chemostats than the GluFruSuc batch conditions. There is also a general trend that PC2 separates on growth rate and all glucose limited chemostats operating at non-Crabtree conditions (i.e. no ethanol production) are collected in lower right quadrant of the scores plot. This view is supported by the loadings plots (Supplementary Figure S4, lower panel) where the growth, substrate and ethanol rates naturally contribute along PC2. Metabolites contributing in PC1 dimension are scattered among the metabolite classes and no pattern is apparent at this level. However, it is worth noting that ATP, ADP, and AMP and G6P are not correlated to growth (orthogonal in loadings plot), and glutamate being a central metabolite in nitrogen metabolism is almost inversely correlated to substrate consumption and ethanol production.

Spearman rank correlation analysis is more suitable for identification of any potential general patterns, with particular focus on correlation between the extracellular rates and intracellular data, the former being fluxes and the latter pool sizes. The analysis was performed on complete data set and localized to the individual five cultivation conditions (1 batch, 4 chemostats). It is rather naïve to expect correlation between the

extracellular rates (growth, substrate and ethanol production) and the global data set levels, and no apparent trends was observed (Supplementary Figure S5), neither much on the individual cultivation conditions either (Supplementary Figures S6-S10), maybe except the observation in N-limited chemostats that citrate and isocitrate are negatively correlated with most other metabolites while α-ketoglutarate, being next in TCA, is slightly positively correlated to many metabolites (Supplementary Figure S9). However, one interesting pattern is that there is little/no correlation within members of same metabolite class, rather individual metabolites have no apparent correlation within class nor pathways but are scattered along the axis on the correlation plots. This contrasts with the noticeable difference in metabolite class variations seen in Supplementary Figure S3, right panel. With these preliminary global interpretations of the data, we now turn to more in-depth analysis with pairwise comparisons among conditions.

Pairwise comparisons. Next, pairwise log2 comparisons were performed to several selected reference conditions: Glucose batch exponential, Glucose batch stationary, LG/HG/ Nlim/ Plim chemostats at 0.12 h-1 dilution rate (Figure 4). Statistical analysis (Two-tailed t-test) for all pairwise comparisons in Panel A- E can be found in Supplementary Table S8). The percentage of significantly changed metabolites ($p<0.05$) is between 50-70% for almost all comparisons, although there were no obvious patterns among the conditions being discovered from this test. However, there are two outliers (Sucrose vs glucose batch exponential growth, and N-lim 0.06 vs 0.12 dilution rates) with less significantly changed metabolites (32 and 23%, respectively).

The metabolite pool composition of fructose and sucrose cultivations are not that different from the glucose batch cultivation (Figure 4 Panel A for exponential cultures and Panel B for stationary phase/ ethanol consuming conditions). Interestingly, G6P, F6P and Pyr pools are quite lower in the fructose cultivation having higher substrate uptake rate and lower ethanol production rate. As expected, most of yeast metabolome on sucrose were in between the range of yeast metabolome on fructose and glucose. However, growth on galactose leads to a different composition of all metabolite classes of the central metabolome. If this is due to the catabolism of galactose directly or indirectly due the 40% reduction in growth rate can't be separated in unlimited batch growth cultivations. The metabolite pools involved in the Leloir pathway for galactose

assimilation were enhanced several folds, while the whole amino acid pool is down regulated (Figure 4 Panel A and Supplementary Figure S11). The latter can be a consequence of the lower growth rate as the amino acids pools also went down in the ethanol consuming stationary phase of the glucose batch cultivation (Figure 4 Panel C, stationary vs exponential glucose batch cultivations). Further for the galactose cultivation; among nucleoside phosphates, all monophosphates were high in concentration. UDP-glu/gal, UDP-Glc/Gal-NAc were nearly 5 and 3-fold higher compared to GluFruSuc cultivated. Intermediates in lower part of glycolysis were down-regulated while PPP metabolites and especially upper glycolytic intermediates were up-regulated several times in comparison to GluFruSuc cultivated yeast. DHAP and F16BP were several folds lower in comparison to GluFruSuc cultivated yeast. Pools of the TCA metabolites citrate, isocitrate and αKG were higher. Interestingly, all metabolite groups except TCA metabolites went down in ethanol consuming phase, the latter pools increased 2-4 times (Figure 4 Panel C).

The overall trends for glucose and nitrogen limited chemostats are increased metabolite pools with increasing growth rate (Figure 4 Panels D-F). In both LG and HG chemostats are most glycolytic, PPP and TCA pools increasing. One difference between high and low glucose is the much larger upregulation of amino acid pools with growth rate in the HG chemostats (Figure 4 Panels D vs E). The HG carbon limited chemostat was characterized by significant reduction in glutamate and the opposite trend with glutamine. This resulted into glutamine as the most dominant amino acid which is like the case of batch culture at exponential phase (Figure 2, Supplementary Table S6). Therefore, glutamine concentration can be viewed as a signature metabolite showing abundance of carbon sources (glucose or fructose) in the medium.

The increase of amino acids pools is even more prominent for the nitrogen limited chemostat series (Figure 4 Panel F). There is also a significant increase in glycolytic and PPP metabolites also. Boer and co-workers (2010) reported that glycolytic intermediates adjust to meet growth requirements and generally have tendency to increase with increased glucose uptake which is confirmed in our study. Interestingly, increased amino acid pools with growth rate is not observed for the phosphate limited chemostats (Figure 4 Panel G), rather the sharp increase in glycolytic and other phosphometabolite pools and decrease of TCA metabolite

pools are the most prominent findings, but note that only low and medium dilution rates were studied under phosphate limited conditions.

Finally, comparing the chosen reference growth rate (0.12 h^{-1}) for the three different nutrient chemostat limitations illuminates an interesting pattern: almost all pools are lower in nitrogen and phosphate limited conditions, except for the TCA metabolites citrate, isocitrate and α-ketoglutarate (Figure 6A and B). F16BP and DHAP is upregulated for the nitrogen-limited condition only.

DISCUSSION

This study provides the most comprehensive collection of central metabolite concentrations over multiple cultivation conditions in *S. cerevisiae*. The findings sometimes confirm previous reports where similar cultivation conditions have been studied, but there are also contradictory results, i.e. we find amino acid pool reduction in nitrogen and phosphate limited chemostats compared to glucose limited, while it was previously reported that glucose and nitrogen limitation were characterized by low amino acids pools and not phosphate limited chemostats (Boer et al 2010). One main reason for this is the chosen LC-MS/MS quantitation strategy and the impressing developments in the mass spectrometry based absolute quantitation methodology the last years. Most previous studies report relative values or quantitation based on a few standards. Here, we employ three LC-MS methods and all analytes are quantified using individual standard curves and ^{13}C-labeled internal standard (either commercially available or application of ^{13}C-glucose yeast extract). Mass spectrometry detection is concentration dependent (the ionization step) and correction with ^{13}C internal standards dramatically increases the precision of the quantitation. In this study we can reliably present and discuss absolute concentrations at the individual and metabolite class levels. That also justifies our revisit to previously reported yeast cultivation conditions, although this study was also expanded with more conditions and better coverage of central metabolite pools. The quantitative Metabolomics methodology has now matured to an advanced level and opening for comprehensive studies of metabolic responses to e.g. stress exposures, gene knock in/out, etc. at the absolute concentration reporting.

Metabolite pool data are challenging to interpret, e.g. metabolite pools can both increase and decrease by increased turnover rates (i.e. flux), but, in any case, any change in metabolite levels indicate perturbation around that specific node/ pathway. The accuracy of the ^{13}C-Internal standard dilution strategy for LC-MS analysis and highest level reproducible microbial cultivation in bioreactors is at the 10-30% relative deviation among technical replicas (resampling from same culture) and 10-20% total among biological replicas (independent cultivations), implying that for single cell microbial model system is more variation introduced during sampling and sample processing and not among independent cultivations[20]. Thus, in total, we can discuss true biological changes at the levels of 30-50% increase and decrease in pools, even for many of the low abundant metabolites, that usually are reported with higher variations.

Energy charge ratio (ECR -the relationship among ATP, ADP and AMP, range 0-1) was consistent and about 0.6 (Supplementary Table S7) across different types of nutrient limitation and specific growth rate[29]. Interestingly, compared to cells grown on other carbon sources, the level of metabolites involved from galactose uptake to its incorporation in glycolysis (also known as Leloir pathway) were increased several folds (Supplementary Figure S11). F1,6BP and DHAP were observed in Crabtree-positive yeasts like our *S. cerevisiae* cen.pk strain to span in the range of 10-fold increase or decrease in concentration which led to the suggestion that these metabolites can potentially function as a general flux indicator of glycolysis and ethanol secretion[2]. These two metabolites also showed the strongest correlation with ethanol production also among our panel of cultivation conditions and metabolite coverage (Supplementary Figure S5). In this regard it is also interesting to note that F1,6BP and DHAP were significantly upregulated in nitrogen vs. glucose limited chemostats (Figure 6A).

Glutamic acid is well known to play a central role in nitrogen metabolism because of its dominance (first or second place) in total amino acids pool irrespective of cultivation conditions, types and severity of nutrient limitation as shown in present study and many previous[30]. α-ketoglutarate, placed at the intersection of carbon and nitrogen metabolic pathways, has also emerged as a key master regulatory metabolite[31] and not only for regulation of carbon metabolism but also nitrogen metabolism[32]. This is also illuminated in the current

metabolite profiling data set when comparing nitrogen vs. glucose limited chemostats (Figure 5A). It is also interesting to note is the sharp accumulation of the three first TCA acids incl α-ketoglutarate in the phosphate limited vs glucose limited chemostat not being reported before to our knowledge (Figure 5B). However, the cultivation data must be included in the interpretation since glucose consumption is almost five times higher in phosphate limited chemostat that also shunts 40% of the glucose carbon to ethanol while there is no ethanol production in the glucose limited chemostat. Biomass yield is however four times higher in the glucose limited chemostat. Altogether this indicates a large re-distribution in the intracellular metabolic fluxes which also is manifested by down-regulation of all metabolite pools except citrate, isocitrate and a-ketoglutarate at same growth rate of phosphate limited vs glucose limited chemostats. Deeper evaluation of the results, e.g. by kinetic model and simulations strictly requires enzyme concentrations[8,33], but various computational approaches have been developed[5]. Experimental determination of main intracellular fluxes using ^{13}C-label studies are also highly desired for validation/ can be used as constraints on modelling and simulation. Such multi-omics studies are extremely resource demanding, but this study shows that the analytical metabolite profiling methodology are ready for such future studies. In all, we have presented the most comprehensive central metabolite pool data set on multiple cultivation conditions, made many interesting observations which are also made available in MetaboLight database for further digestion.

DECLARATIONS

All co-authors consent to publishing the content of this publication.

Metabolite abbreviations can be found in Supplementary Table S6.

Conflict of interest

The authors declare that the research was conducted in the absence of any commercial or financial relationships that could be construed as a potential conflict of interest.

Author contributions

KK and PB designed the study. KK performed the cultivations, sampling and analysis. KK, VV and PB were involved in data analysis, presentation and interpretation of the results and writing of the manuscript. PB was responsible for funding acquisition and project administration.

Funding

This work was funded by internal sources at NTNU and as a part of the Era-IB project Terpenosome (Research Council of Norway grant no. 237165) and the Digital Life Norway project InBioPharm (Research Council of Norway grant no. 248885).

Availability of data and materials

All metabolite data are available in MetaboLights database with accession number: (will be done after acceptance and prior to publishing,)

Acknowledgements

Centre for Digital Life Norway is thanked for administrative support during the study. NV-faculty Mass Spectrometry facility is thanked for support during all MS analysis, and technical help from Simen Liberg Tronsaune, Ida Eide Langørgen and Marit Hallvardsdotter Stafsnes is highly appreciated.

Supplementary Materials

Supplementary information accompanies this paper at: link to be added.

FIGURE LEGENDS

Figure 1. Offline and online cultivation data for Batch (A), Low Glucose limited chemostat (B), High Glucose limited chemostat (C), Nitrogen limited chemostat (D), and Phosphate limited chemostat (E). Units for the Yield (Y) and specific rates (q) are given in the text box. RQ is the respiratory coefficient (ratio of CO_2 production and O_2 consumption).

Figure 2. Heat-map showing abundance of individual intracellular metabolite concentration represented in logarithmic scale across different cultivation conditions in batch and chemostat.

Figure 3. Upper bar diagram shows the abundance of group of intracellular metabolites concentration and lower bar diagram shows the relative fraction of metabolites pools represented in terms of percentage.

Figure 4. Panels A to G shows relative metabolite concentrations at log2 scale vs. glucose batch cultivation and dilution rate of 0.12 h^{-1} for chemostat cultivations (for individual nutrient limitations). Max values for color formatting are set to -3 and 3.

Figure 5. A plot showing changes in the metabolites of central metabolic pathways. This plot is plotted based on logarithmic value (base 2) of ratio of intracellular metabolites concentration of *S.cerevisiae* in **A)** nitrogen to glucose and **B)** phosphorous to glucose limited chemostat at dilution rate of 0.12 h^{-1}. Heatmap coding is from – max (blue) to max (red), below LOQ/uncertain/ not detected metabolites are grey.

REFERENCES

1 Zimmerman, F. K. & Entian, K. D. *Yeast sugar metabolism: Biochemistry, Genetics, Biotechnology and Applications*. (Technomic Publishing Company Inc, 1997).

2 Christen, S. & Sauer, U. Intracellular characterization of aerobic glucose metabolism in seven yeast species by 13C flux analysis and metabolomics. *Fems Yeast Research* **11**, 263-272, doi:10.1111/j.1567-1364.2010.00713.x (2011).

3 Kapoore, R. V. & Vaidyanathan, S. Towards quantitative mass spectrometry-based metabolomics in microbial and mammalian systems. *Philos. Trans. R. Soc. A-Math. Phys. Eng. Sci.* **374**, doi:10.1098/rsta.2015.0363 (2016).

4 Becker, J. & Wittmann, C. From systems biology to metabolically engineered cells - an omics perspective on the development of industrial microbes. *Curr. Opin. Microbiol.* **45**, 180-188, doi:10.1016/j.mib.2018.06.001 (2018).

5 Bordbar, A. *et al.* Elucidating dynamic metabolic physiology through network integration of quantitative time-course metabolomics. *Scientific Reports* **7**, 12, doi:10.1038/srep46249 (2017).

6 Dikicioglu, D., Pir, P. & Oliver, S. G. Predicting complex phenotype-genotype interactions to enable yeast engineering: Saccharomyces cerevisiae as a model organism and a cell factory. *Biotechnol. J.* **8**, 1017-U1080, doi:10.1002/biot.201300138 (2013).

7 Bennett, B. D. *et al.* Absolute metabolite concentrations and implied enzyme active site occupancy in Escherichia coli. *Nature Chemical Biology* **5**, 593-599, doi:10.1038/nchembio.186 (2009).

8 Smallbone, K. *et al.* A model of yeast glycolysis based on a consistent kinetic characterisation of all its enzymes. *Febs Letters* **587**, 2832-2841, doi:10.1016/j.febslet.2013.06.043 (2013).

9 de Ruijter, J. C., Koskela, E. V., Nandania, J., Frey, A. D. & Velagapudi, V. Understanding the metabolic burden of recombinant antibody production in Saccharomyces cerevisiae using a quantitative metabolomics approach. *Yeast* **35**, 331-341, doi:10.1002/yea.3298 (2018).

10 Martinez, V. S. & Kromer, J. O. Quantification of Microbial Phenotypes. *Metabolites* **6**, 24, doi:10.3390/metabo6040045 (2016).

11 Nielsen, J. & Keasling, J. D. Engineering Cellular Metabolism. *Cell* **164**, 1185-1197, doi:10.1016/j.cell.2016.02.004 (2016).

12 Guo, A. C. *et al.* ECMDB: The E-coli Metabolome Database. *Nucleic Acids Research* **41**, D625-D630, doi:10.1093/nar/gks992 (2013).

13 Jewison, T. *et al.* YMDB: the Yeast Metabolome Database. *Nucleic Acids Research* **40**, D815-D820, doi:10.1093/nar/gkr916 (2012).

14 Wishart, D. S. *et al.* HMDB: the human metabolome database. *Nucleic Acids Research* **35**, D521-D526, doi:10.1093/nar/gkl923 (2007).

15 Sansone, S. A. *et al.* The metabolomics standards initiative. *Nature Biotechnology* **25**, 844-848, doi:10.1038/nbt0807-846b (2007).

16 Edison, A. S. *et al.* The Time Is Right to Focus on Model Organism Metabolomes. *Metabolites* **6**, doi:10.3390/metabo6010008 (2016).

17 Kvitvang, H. F. N., Kristiansen, K. A. & Bruheim, P. Assessment of capillary anion exchange ion chromatography tandem mass spectrometry for the quantitative profiling of the phosphometabolome and organic acids in biological extracts. *Journal of Chromatography A* **1370**, 70-79, doi:10.1016/j.chroma.2014.10.029 (2014).

18 Rost, L. M., Shafaei, A., Fuchino, K. & Bruheim, P. Zwitterionic HILIC tandem mass spectrometry with isotope dilution for rapid, sensitive and robust quantification of pyridine nucleotides in biological extracts. *Journal of Chromatography B-Analytical Technologies in the Biomedical and Life Sciences* **1144**, doi:10.1016/j.jchromb.2020.122078 (2020).

19 Stafsnes, M. H., Rost, L. M. & Bruheim, P. Improved phosphometabolome profiling applying isotope dilution strategy and capillary ion chromatography-tandem mass spectrometry. *Journal of*

Chromatography B-Analytical Technologies in the Biomedical and Life Sciences **1083**, 278-283, doi:10.1016/j.jchromb.2018.02.004 (2018).

20 Rost, L. M. *et al.* Absolute Quantification of the Central Carbon Metabolome in Eight Commonly Applied Prokaryotic and Eukaryotic Model Systems. *Metabolites* **10**, doi:10.3390/metabo10020074 (2020).

21 Schaechter, M., Maaloe, O. & Kjeldgaard, N. O. Dependency on medium and temperature of cell size and chemical composition during balances growth of Salmonella typhimurium. *Journal of General Microbiology* **19**, 592-606, doi:10.1099/00221287-19-3-592 (1958).

22 van Dijken, J. P. *et al.* An interlaboratory comparison of physiological and genetic properties of four Saccharomyces cerevisiae strains. *Enzyme Microb. Technol.* **26**, 706-714, doi:10.1016/s0141-0229(00)00162-9 (2000).

23 Boer, V. M., Crutchfield, C. A., Bradley, P. H., Botstein, D. & Rabinowitz, J. D. Growth-limiting Intracellular Metabolites in Yeast Growing under Diverse Nutrient Limitations. *Molecular Biology of the Cell* **21**, 198-211, doi:10.1091/mbc.E09-07-0597 (2010).

24 Nishino, S., Okahashi, N., Matsuda, F. & Shimizu, H. Absolute quantitation of glycolytic intermediates reveals thermodynamic shifts in Saccharomyces cerevisiae strains lacking PFK1 or ZWF1 genes. *J. Biosci. Bioeng.* **120**, 280-286, doi:10.1016/j.jbiosc.2015.01.012 (2015).

25 Jung, Y. H., Kim, S., Yang, J., Seo, J. H. & Kim, K. H. Intracellular metabolite profiling of Saccharomyces cerevisiae evolved under furfural. *Microb. Biotechnol.* **10**, 395-404, doi:10.1111/1751-7915.12465 (2017).

26 Moktaduzzaman, M. *et al.* Galactose utilization sheds new light on sugar metabolism in the sequenced strain Dekkera bruxellensis CBS 2499. *Fems Yeast Research* **15**, doi:10.1093/femsyr/fou009 (2015).

27 Lis, A. V. *et al.* Exploring small-scale chemostats to scale up microbial processes: 3-hydroxypropionic acid production in S. cerevisiae. *Microb. Cell. Fact.* **18**, doi:10.1186/s12934-019-1101-5 (2019).

28 Daran-Lapujade, P. *et al.* Role of transcriptional regulation in controlling fluxes in central carbon metabolism of Saccharomyces cerevisiae - A chemostat culture study. *Journal of Biological Chemistry* **279**, 9125-9138, doi:10.1074/jbc.M309578200 (2004).

29 Atkinson, D. E. & Walton, G. M. Adenosine triphosphate conservation in metabolic regulation - Rat liver citrate cleavage enzyme. *Journal of Biological Chemistry* **242**, 3239-& (1967).

30 Watson, T. G. Amino-Acid Pool Composition of Saccharomyces-Cerevisiae as a Function of Growth-Rate and Amino-Acid Nitrogen-Source. *Journal of General Microbiology* **96**, 263-268, doi:10.1099/00221287-96-2-263 (1976).

31 Huergo, L. F. & Dixon, R. The Emergence of 2-Oxoglutarate as a Master Regulator Metabolite. *Microbiology and Molecular Biology Reviews* **79**, 419-435, doi:10.1128/mmbr.00038-15 (2015).

32 Chubukov, V., Gerosa, L., Kochanowski, K. & Sauer, U. Coordination of microbial metabolism. *Nat. Rev. Microbiol.* **12**, 327-340, doi:10.1038/nrmicro3238 (2014).

33 Hameri, T., Fengos, G., Ataman, M., Miskovic, L. & Hatzimanikatis, V. Kinetic models of metabolism that consider alternative steady-state solutions of intracellular fluxes and concentrations. *Metabolic Engineering* **52**, 29-41, doi:10.1016/j.ymben.2018.10.005 (2019).

Figures

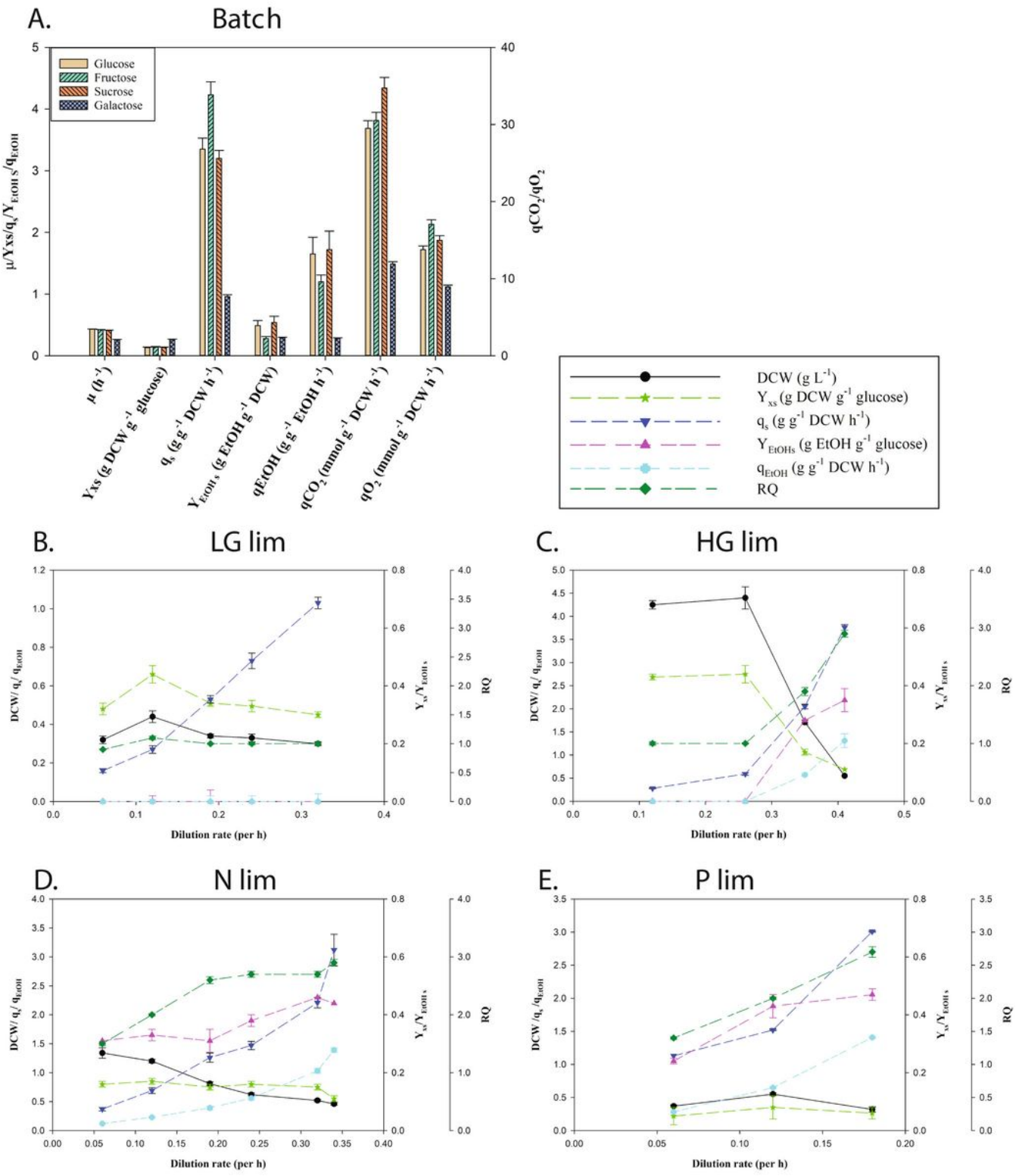

Figure 1

Offline and online cultivation data for Batch (A), Low Glucose limited chemostat (B), High Glucose limited chemostat (C), Nitrogen limited chemostat (D), and Phosphate limited chemostat (E). Units for the Yield

(Y) and specific rates (q) are given in the text box. RQ is the respiratory coefficient (ratio of CO2 production and O2 consumption).

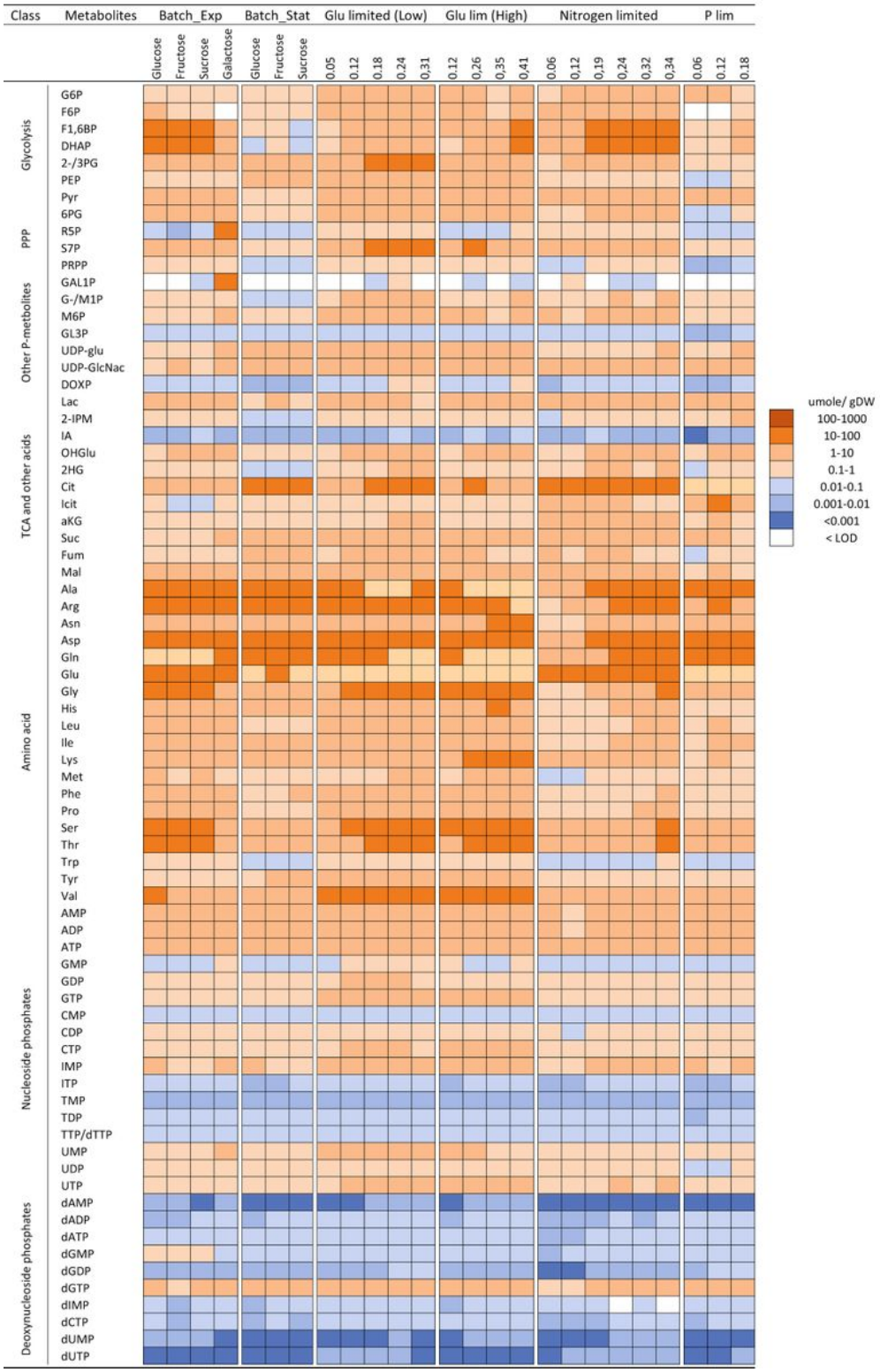

Figure 2

Heat-map showing abundance of individual intracellular metabolite concentration represented in logarithmic scale across different cultivation conditions in batch and chemostat.

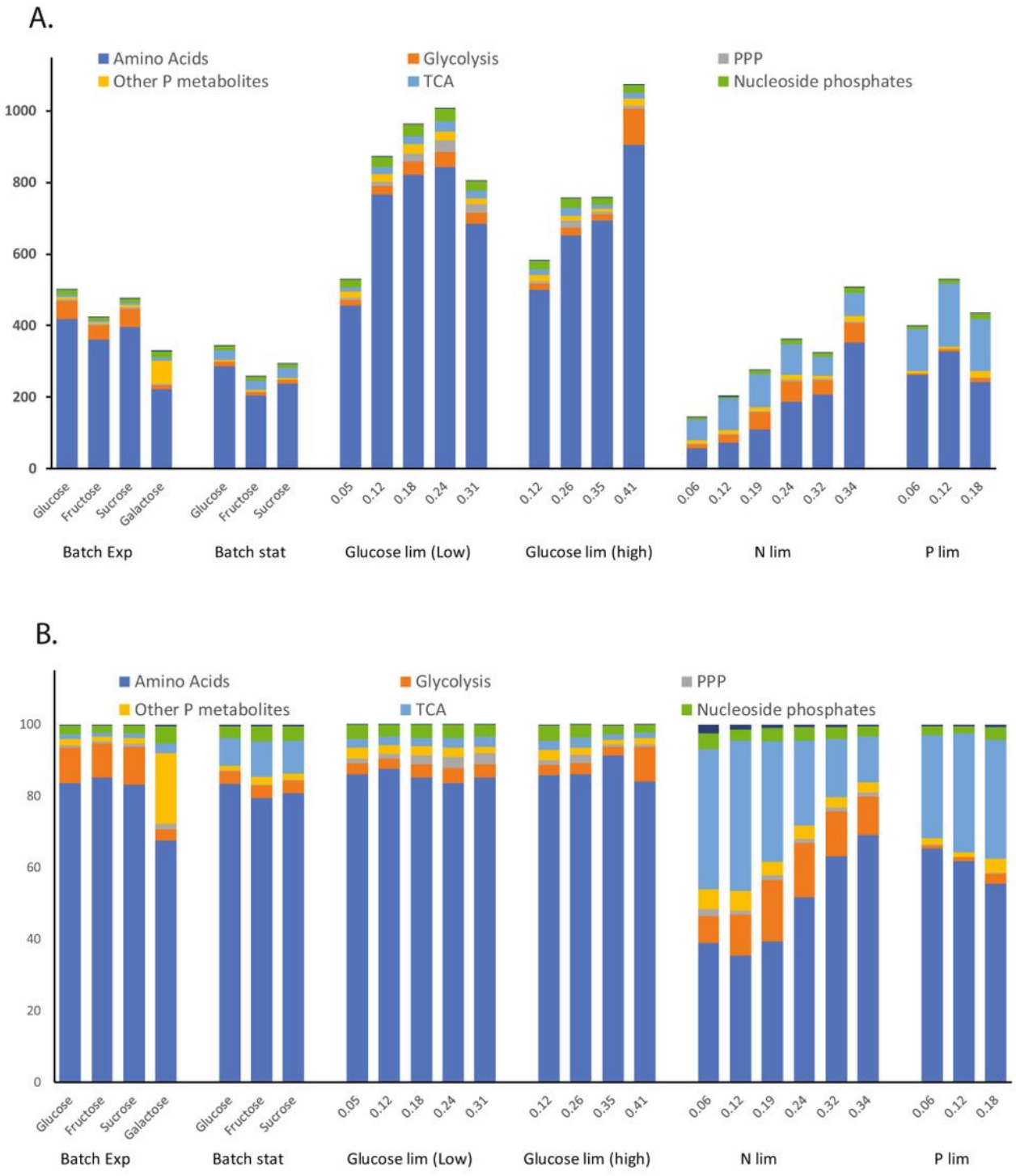

Figure 3

Upper bar diagram shows the abundance of group of intracellular metabolites concentration and lower bar diagram shows the relative fraction of metabolites pools represented in terms of percentage.

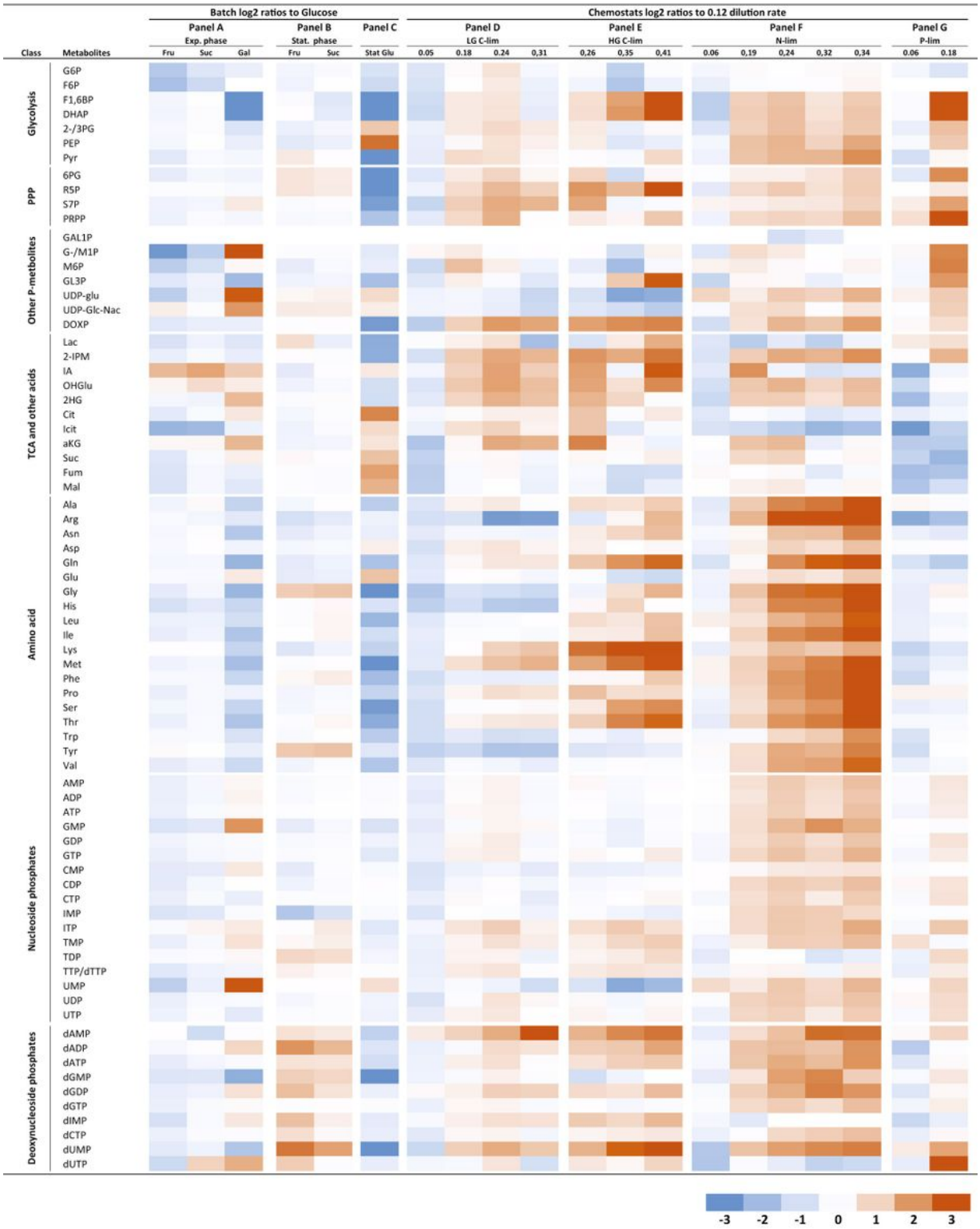

Figure 4

Panels A to G shows relative metabolite concentrations at log2 scale vs. glucose batch cultivation and dilution rate of 0.12 h-1 for chemostat cultivations (for individual nutrient limitations). Max values for color formatting are set to -3 and 3.

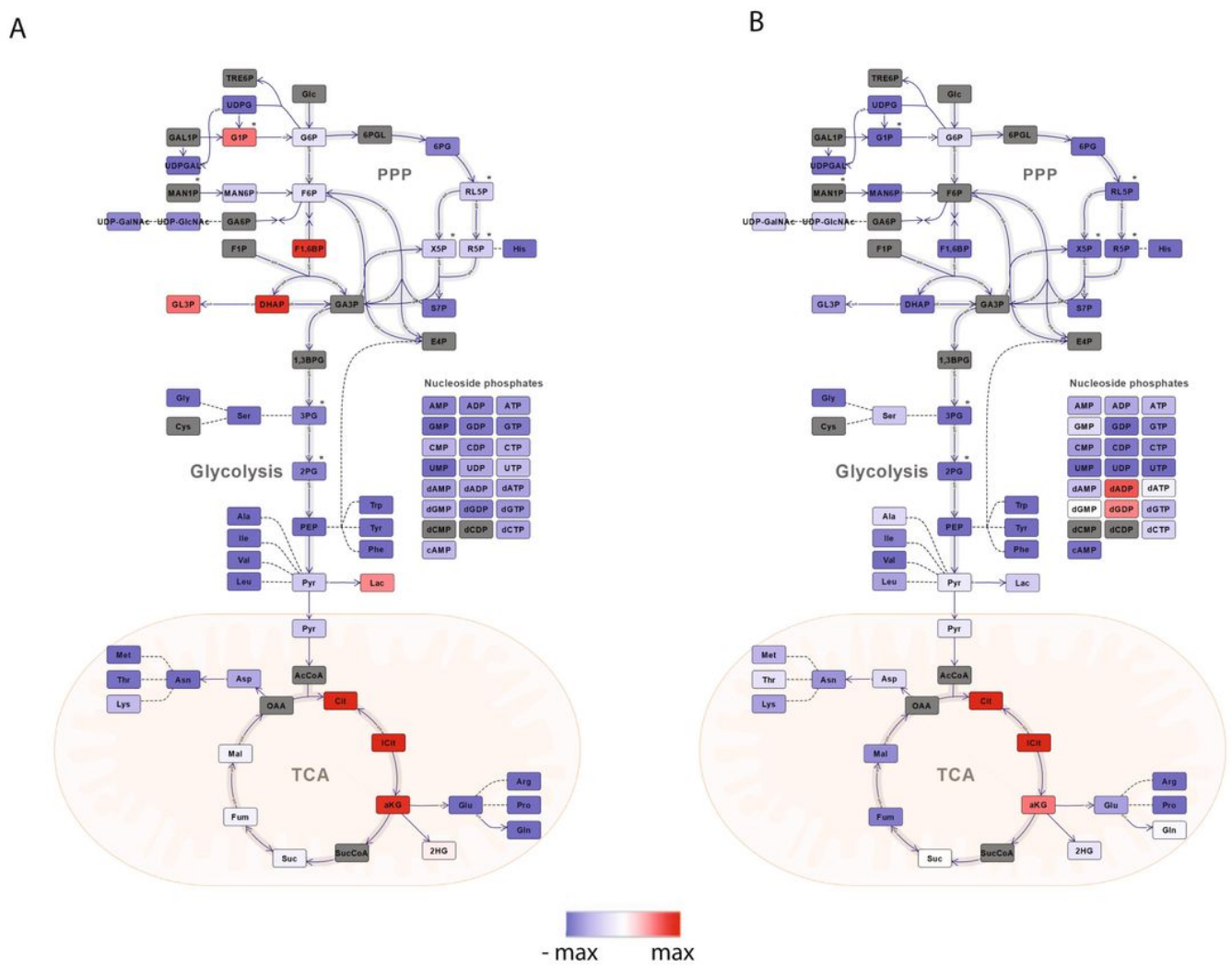

Figure 5

A plot showing changes in the metabolites of central metabolic pathways. This plot is plotted based on logarithmic value (base 2) of ratio of intracellular metabolites concentration of S.cerevisiae in A) nitrogen to glucose and B) phosphorous to glucose limited chemostat at dilution rate of 0.12 h-1. Heatmap coding is from – max (blue) to max (red), below LOQ/uncertain/ not detected metabolites are grey.

Supplementary Files

This is a list of supplementary files associated with this preprint. Click to download.

- SupplementaryFigures.docx
- SupplementaryTablesS15.docx
- SupplementaryTableS6.xlsx
- SupplementaryTableS7.xlsx
- SupplementaryTableS8.xlsx